crystals

MDPI

Article

One-Step Synthesis of Cu–ZnO@C from a 1D Complex $[Cu_{0.02}Zn_{0.98}(C_8H_3NO_6)(C_{12}H_8N_2)]_n$ for Catalytic Hydroxylation of Benzene to Phenol

Guanghui Wang [1], Zheng Yan [2,3], Li Song [2], Lei Li [2,*], Jie Zhu [2] and Haidong Wang [2,*]

1 School of Petrochemical Engineering, Changzhou University, Changzhou 213164, China; 18257341699@163.com
2 College of Biological, Chemical Sciences and Engineering, Jiaxing University, Jiaxing 314001, China; yzheng158@163.com (Z.Y.); songli@mail.zjxu.edu.cn (L.S.); zhuyaojie1113@163.com (J.Z.)
3 Laboratory for Preparation and Application of Ordered Structural Materials of Guangdong Province, Shantou University, Shantou 515063, China
* Correspondence: leili@mail.zjxu.edu.cn (L.L.); whdoctor@mail.zjxu.edu.cn (H.W.); Tel.: +86-573-8364-3852 (L.L. & H.W.)

Received: 3 May 2018; Accepted: 14 May 2018; Published: 16 May 2018

Abstract: A novel one-dimensional bimetallic complex $[Cu_{0.02}Zn_{0.98}(C_8H_3NO_6)(C_{12}H_8N_2)]_n$ ("Complex") has been synthesized by a hydrothermal method. A Cu–ZnO@C composite was obtained by a one-step pyrolysis of Complex. Correlated with the characterization results, it is confirmed that both metallic Cu^0 and ZnO nanoparticles were highly dispersed on/in the carbon substrate. This simple one-step pyrolysis method avoids the high-temperature pretreatment under H_2 commonly required for preparation of such Cu–ZnO catalysts. The Cu–ZnO@C composite was tested with respect to its catalytic activities for the hydroxylation of benzene to phenol with H_2O_2. The results indicate that the benzene conversion, phenol yield, and phenol selectivity reached the maximum values (55.7%, 32%, and 57.5%, respectively) at Complex carbonized at 600 °C, and were higher than those of the commercial mixed sample. Compared with the other candidate catalysts, the turnover frequency (TOF) of our Cu–ZnO@C catalyst (117.9 mmol mol^{-1} s^{-1}) can be ranked at the top. The higher catalytic activities should be due to the highly dispersed metallic Cu^0 and ZnO particles as well as their synergistic interaction.

Keywords: metal organic frameworks; carbonization; Cu–ZnO; hydroxylation of benzene

1. Introduction

Metal organic frameworks (MOFs) have received considerable attentions because of their large surface area, low framework density, and high pore volume. As for typical porous materials, the applications of MOFs have been extensively explored in sensors [1], heterogeneous catalysts [2], gas adsorption/separation [3,4], hydrogen storage, and the stationary phase in chromatography.

Owing to the controllable structures of MOFs [5], they can be used as both precursors and templates to purposefully prepare advanced functional materials, such as metal oxide@C nanomaterials and porous carbon materials [6,7]. Xu et al. firstly communicated that MOFs can be used as precursors to synthesize porous carbon materials [8]. Furthermore, high-surface-area carbon materials derived from MOFs have been extended to the application of electrochemistry [9]. Impressively, previous works have indicated that metal ions and morphology of MOFs were varied to engineer the crystallinity and morphology of carbon materials [10]. Moreover, the mixed-metal MOF materials can be fabricated

by replacing a portion of the metal cations with other similar metal cations. Then, the mixed-metal oxides (or solid solutions) can be obtained after a carbonization process [11].

As typical transition metals, copper and zinc are usually considered as good candidates for heterocatalytic reactions. Nevertheless, there is an argument regarding the role of metallic Cu^0, Cu^+, and Cu^{2+} in catalytic reactions, such as photocatalytic hydrogen generation [12] or water–gas shift reactions [13]. For this reason, it is important to purposefully control the desired valence of copper species. Unfortunately, CuO species are usually obtained [14–16], while the preparations of metallic Cu^0 or Cu_2O need further reduction. For example, CuO supported on ZnO was commonly prepared by homogeneous coprecipitation, deposition–precipitation, and conventional coprecipitation methods. However, to prepare metallic Cu supported on ZnO, the obtained CuO–ZnO composite oxides should be further reduced under H_2 [17,18]. Even when the metallic Cu was used as the copper source to support ZnO, metallic Cu finally changed to CuO, and then CuO–ZnO composite was formed [19]. Therefore, there is an urgent requirement for the preparation of metallic Cu^0 supported on ZnO by a simple one-step method.

In the present work, a novel one-dimensional bimetallic complex $[Cu_{0.02}Zn_{0.98}(C_8H_3NO_6)(C_{12}H_8N_2)]_n$ has been successfully prepared and characterized. The Complex was directly pyrolyzed under N_2 to remove organic groups and synthesize Cu–ZnO@C composites, which are composed of metallic Cu^0, ZnO, and carbon. Finally, the Cu–ZnO@C composite was tested with respect to its catalytic activities for the hydroxylation of benzene to phenol with H_2O_2.

2. Materials and Methods

2.1. Chemicals

Copper acetate ($Cu(OAc)_2 \cdot H_2O$, ≥98%), zinc acetate dehydrate ($Zn(OAc)_2 \cdot 2H_2O$, ≥98%), methanol (CH_3OH, ≥99.5%), sodium hydroxide (NaOH, ≥96%), 5-nitroisophthalato (nip) (≥98%), and 1,10-phenanthroline (phen) (≥98%) were all purchased from Shanghai Chemical Reagent Ltd. All chemicals were used without further purification or drying.

2.2. Preparation of Complex

$Cu(OAc)_2 \cdot H_2O$ (0.3998 g, 2 mmol), $Zn(OAc)_2 \cdot 2H_2O$ (0.4392 g, 2 mmol), NaOH (0.1223 g, 3 mmol), 1,10-phenanthroline (0.7916 g, 4 mmol), 5-nitroisophthalato (0.8363 g, 4 mmol), 24 mL deionized water, and 24 mL methanol were mixed together in a 180 mL Teflon-lined autoclave and stirred for 45 min at room temperature. The crystallization was kept on 160 °C for 144 h. After cooling down to room temperature, the resulting stone-yellow precipitate was filtered and washed five times with a mixed solution of deionized water and methanol (v/v = 4:1). The obtained material was dried in a vacuum at 70 °C for 5 h. Theoretical and found results of elemental analyses (%) are as follows: Theoretical: C, 52.99; H, 2.43; N, 9.27. Found: C, 52.95; H, 2.39; N, 9.29. The found data are almost identical with the theoretical data. The ratio of copper and zinc elements is about 1:62. The main FTIR bonds in the KBr discs are as follows: 3432(s), 3101(m), 1634(vs), 1622(s), 1568(w), 1532(s), 1457(m), 1428(m), 1345(s), 1300(vs), 1182(m), 1082(w), 920(w), 845(s), 786(m), 729(s), 646(w), 550(w), 410(w).

2.3. Experimental Instruments

X-ray diffraction analysis data was collected with an Oxford Diffraction Gemini R Ultra diffractometer (Westchem Mfg. Ltd., Abbotsford, BC, Canada) with graphite-monochromated Mo-Kα ray (λ = 0.71073 Å) at 296 K. Elemental analyses (C, H and N) were performed on a Carlo-Erba model 1106 elemental analyzer (Carlo Erba, Milano, Italy). The actual copper and zinc contents in Complex were measured by ICP-OES using a Varian 710-ES analyzer (Varian, Palo Alto, CA, USA). FTIR spectra was collected on a FTIR-NEXUS 470 spectrometer (Thermo Nicolet Corporation, Madison, WI, USA). Powder X-ray diffraction (powder XRD) data were recorded by a Bruker D8 (Bruker, Billerica, MA, USA) equipped with Cu-Kα (λ = 0.1541 nm) radiation operating at 40 kV

and 40 mA. The X-ray photoelectron spectroscopy (XPS) measurements were carried out by a VG ESCALAB 250 spectrophotometer (Thermo Electron, Waltham, MA, USA) with Al-Kα radiation (1486.6 eV), operating at 15 kV × 10 mA and kept at 1×10^{-9} mbar. All binding energies (BE) were calibrated by using that of C 1 s (284.5 eV). Thermogravimetric (TG) analysis was performed on a Simultaneous TG-DTA/ DSC-Apparatus 409 PC (STA 409 PC) instrument (Netzsch Group, Selb, Germany) under an N_2 atmosphere with a 10 °C min^{-1} warming rate. Scanning electron microscopy (SEM) was carried out by a Hitachi S-4800 instrument (Hitachi, Tokyo, Japan) operating at 20 kV. Energy dispersive spectrometer (EDS) analysis was performed on a KEVEX-Sigma energy dispersive spectrometer (Hitachi, Tokyo, Japan). High performance liquid chromatography (HPLC) was analyzed in an Agilent 1200 liquid chromatograph (Agilent, Santa Clara, CA, USA) equipped with a ZORBAX Eclipse XDB-C18 column (Agilent, Santa Clara, CA, USA). HPLC conditions: mobile phase: CH_3OH/H_2O = 30:70 (*v*/*v*), flow rate: 1.0 mL min^{-1}, detector wavelength: 270 nm, sample dose: 20 μL.

2.4. Evaluation of Catalytic Activity

The typical evaluation of catalytic activity is described as follows (Scheme 1) [20,21]: 40 mg of catalysts were dispersed in 1.8 mL (20 mmol) of benzene and 6 mL of 99.8 wt % acetonitrile solvent. When temperature came up to 70 °C, 4.08 mL (40 mmol) of 30 wt % hydrogen peroxide was slowly added dropwise. This reaction was maintained for 6 h. The hydroxylation reaction liquid of phenol was measured as about 1.0 mL and diluted 10 times. The diluted liquid was filtered by the 0.22 μm cellulose acetate filter to remove catalysts. The remaining reactants and obtained products were analyzed by HPLC. Benzene conversion and phenol selectivity were calculated as follows:

$$\text{Benzene Conversion \%} = 100\% - \frac{n_B}{n_{Bo}} \times 100\%$$

$$\text{Phenol Selectivity \%} = \frac{n_p}{n_p + n_h} \times 100\%$$

$$\text{Phenol Yield \%} = \text{Benzene Conversion \%} \times \text{Phenol Selectivity \%}$$

where n_B is the amount of benzene (mmol), n_{Bo} is the amount of original benzene (mmol), n_P is the amount of phenol (mmol), and n_h is the amount of hydroquinone (mmol).

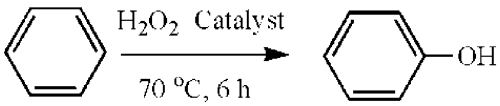

Scheme 1. Hydroxylation of benzene to phenol with H_2O_2.

3. Results and Discussion

3.1. Single Crystal X-ray Data Collection of Complex

The structure was analyzed by direct methods and refined on F^2 by a full-matrix least-squares methods using the SHELXTL package [22]. The crystal data and structure refinements of Complex are listed in Table 1. Selected bond lengths and angles are shown in Table 2. Crystallographic data for Complex have been deposited in the Cambridge Crystallographic Data Center (CCDC): its crystal structures can be obtained with the CCDC reference number: 1817133. To enable synergistic catalysis, a novel bimetallic complex $[Cu_{0.02}Zn_{0.98}(C_8H_3NO_6)(C_{12}H_8N_2)]_n$ has been successfully synthesized, which is isostructural to the previously communicated monometallic Zn–MOF (No. 601347, space group of *C*2/*c*, Cambridge Crystallographic Data Centre) [23].

Table 1. Crystallographic data of Complex.

Parameter	Complex
Empirical formula	$Cu_{0.02}Zn_{0.98}C_{20}H_{11}N_3O_6$
Formula weight	454.68
Temperature (K)	296
Crystal system	Monoclinic
Space group	*C*2/*c*
a (Å)	28.797 (6)
b (Å)	9.2757 (19)
c (Å)	14.965 (3)
α (°)	90
β (°)	115.58 (3)
γ (°)	90
Volume (Å^3)	3605.4 (13)
Z	8
D (calc) (g cm^{-3})	1.669
Crystal size (mm)	0.29 × 0.21 × 0.17
Ref. collected	3572
Ref. unique	2774
R_{int}	0.0307
GOF	1.031
Completeness (%)	100.00
R_1 [a] (*I* > 2*σ*(*I*))	0.0456
wR_2 [b] (*all data*)	0.1413

[a] $R_1 = \sum ||F_o| - |F_c|| / \sum |F_o|$; [b] $wR_2 = \{[\sum w(F_o^2 - F_c^2)^2] / \sum [w(F_o^2)^2]\}^{1/2}$. CCDC: 1817133.

Table 2. Selected bond lengths (Å) and angles (°) for Complex.

Complex	Bond Lengths (Angles)	Complex	Bond Lengths (Angles)
Zn(Cu)1–O1	1.929 (2)	Zn(Cu)1–O3 [i]	2.015 (2)
Zn(Cu)1–O4 [i]	2.433 (3)	Zn(Cu)1–N2	2.055 (3)
Zn(Cu)1–N3	2.072 (3)	-	-
O1–Zn(Cu)1–O3 [i]	106.37 (11)	O1–Zn(Cu)1–O4 [i]	87.21 (10)
O1–Zn(Cu)1–N2	115.98 (11)	O1–Zn(Cu)1–N3	118.44 (11)
O3 [i]–Zn(Cu)1–O4 [i]	58.45 (9)	O3 [i]–Zn(Cu)1–N2	123.41 (10)
O3 [i]–Zn(Cu)1–N3	109.98 (10)	O4 [i]–Zn(Cu)1–N2	87.17 (9)
O4 [i]–Zn(Cu)1–N3	154.35 (10)	N2–Zn(Cu)1–N3	81.38 (11)

Symmetry codes: [i] x, −y, z + 1/2.

3.2. Description of Crystal Structure

Single crystal X-ray diffraction analysis reveals that Complex crystallizes in the monoclinic space group *C*2/*c* (Table 1). Each independent crystallographic unit consists of one crystallographically independent site of Zn(Cu), one phen ligand, and one nip ligand. Each zinc(copper) atom in Complex resides in a triangular bipyramid geometry, where it is ligated by N(2), O(1), and O(3) atoms in the equatorial plane and N(3) and O(4) in the axial position (Figure 1). Zn(Cu) is coordinated with the equatorial positions occupied by two carboxylato-oxygen atoms ((Zn(Cu)–O1) = 1.929 Å, (Zn(Cu)–O3) = 2.015 Å) and one nitrogen (N(2)) of the phen (Zn(Cu)–N2) = 2.055 Å). The axial positions occupied by one carboxylato-oxygen (O(4)) ((Zn(Cu)–O4) = 2.433 Å) and one nitrogen (N(3)) of the phen (Zn(Cu)–N3) = 2.072 Å). Evidently, the equatorial Zn(Cu)–O and Zn(Cu)–N distances are shorter than the axial distances. Along the *c*-axis direction, the adjacent Zn(Cu) atoms are linked by nip ligands into a one-dimensional chain structure, with an Zn(Cu)···Zn(Cu) separation of 9.910 Å. All the nip ligands in Complex adopt the monodentate/bidentate coordination mode, and the two aromatic rings of the adjacent nip ligands have a dihedral angle of 84.83°. The plane–plane distance between two phen ligands of adjacent chains is around 3.653 Å, indicating π–π stacking interactions, by which

consecutive chains are further packed into 1D supramolecular double-chains in Complex as shown in Figure 2.

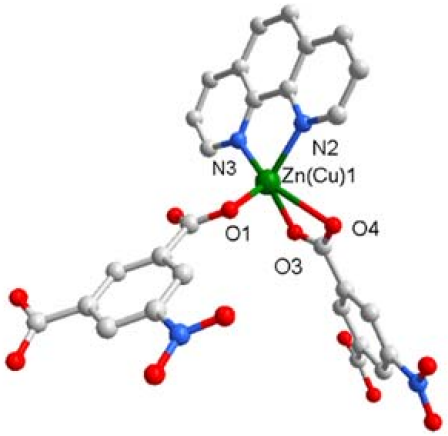

Figure 1. Coordination geometries of Complex.

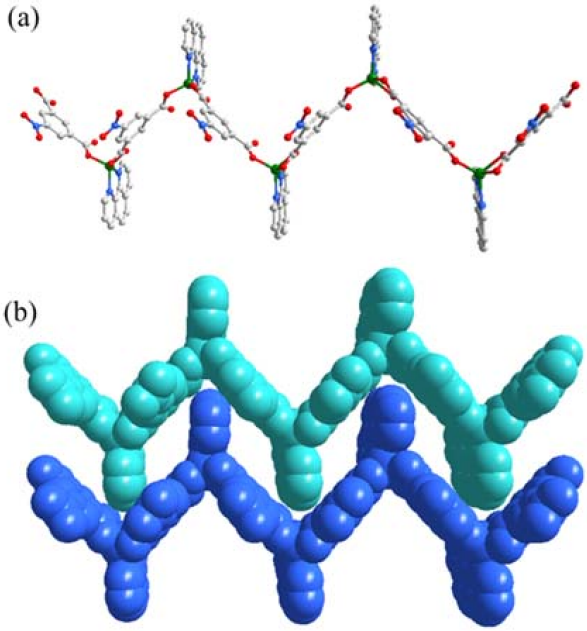

Figure 2. The infinite 1D zigzag chain of Complex (**a**); the 1D supramolecular double-chain in Complex (**b**).

3.3. Characterization

As presented in Figure 3, the experimental powder XRD pattern of Complex matched well with the simulative pattern determined from the single-crystal XRD experiment, indicating that a pure Complex was obtained. The FTIR spectra of the as-synthesized Complex were also carried out. Based on the literature [23], the wide band at about 3432 cm^{-1} is related to the OH stretching vibrations. The C–H stretches are observed at 3101 cm^{-1}. The bands at 1532 and 1345 cm^{-1} are attributed to the vibrations of N=O in the nitro group. The band of C=N appears at 1634 cm^{-1}. The band at 1082 cm^{-1} is derived from the vibrations of C–N in the nitro group of benzene. The absorption at 410 cm^{-1} are ascribed to the stretching vibrations of the Zn–O or Cu–O groups, indicating that coordinate bonds had been formed. All above bands are consistent with the single crystal structural analysis.

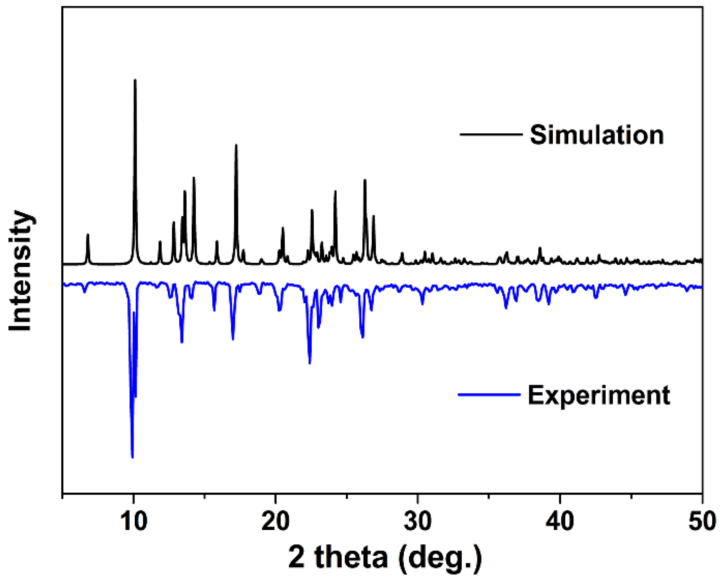

Figure 3. Experimental and simulative powder XRD patterns of Complex.

In order to prepare porous carbon and metal oxide composite nanomaterials, Complex was annealed at 600 °C under N_2 to remove the organic groups. As presented in Figure 4, the powder XRD pattern indicates that the compound consists of the metallic Cu^0, ZnO, and carbon. Furthermore, the XPS survey spectrum suggests that the compound is composed of the elements of Cu, Zn, O, C, and N, as shown in Figure 4. Hereinto, the remaining N should be due to the uncompleted pyrolysis, because the hydrolysis temperature of 600 °C is lower than the 800 °C temperature in TG analysis. For Cu 2p and Zn 2p spectra, Cu and Zn elements present as metallic Cu^0 and Zn^{2+}, respectively, as shown in Figure 5b,d.

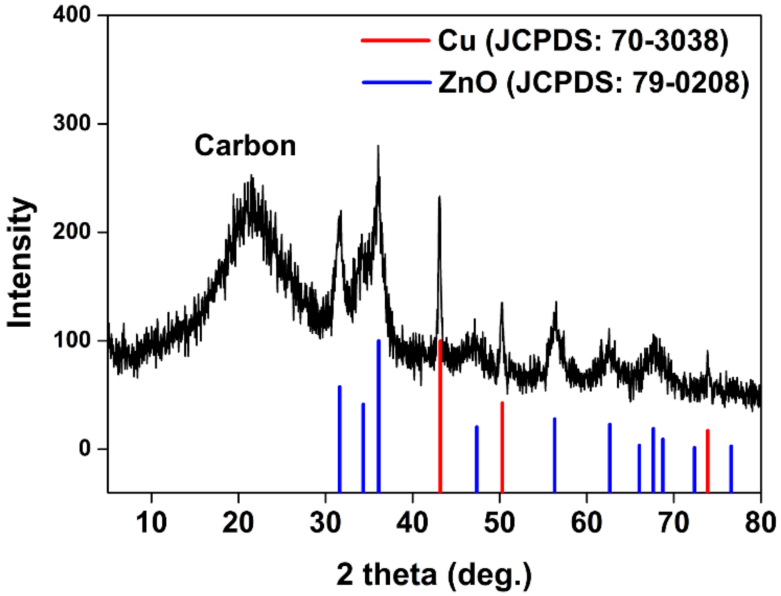

Figure 4. Powder XRD pattern of the Cu–ZnO@C compound prepared by heat-treated Complex at 600 °C under N_2.

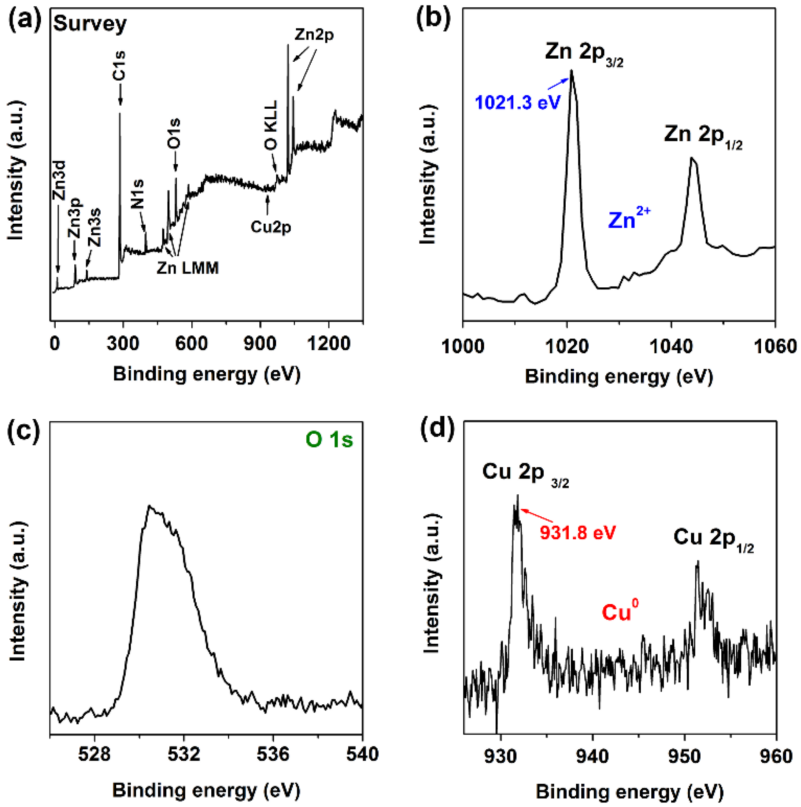

Figure 5. XPS of the Cu–ZnO@C compound prepared by heat-treated Complex at 600 °C under N_2. (**a**) Survey; (**b**) Zn 2p; (**c**) O 1s; (**d**) Cu 2p.

As described in the crystal structure, there are bivalent Cu^{2+} cations in the as-synthesized Complex. Thus, the bivalent Cu^{2+} was reduced to metallic Cu^0 during the carbonization process under N_2. The reduction of Cu^{2+} to Cu^0 might be ascribed to the following two explanations: Firstly, the coordination N atoms are stronger reductants compared with O atoms because N atoms have weaker electronegativity than O atoms. Thus, coordination N atoms possibly provide electrons for Cu^{2+} to form metallic Cu^0. Secondly, if copper firstly existed as CuO just like ZnO in the obtained Cu–ZnO@C compound, the remained abundant carbon might reduce CuO to metallic Cu^0 under high temperatures as in the following chemical reaction:

$$C + CuO \underset{N_2}{\overset{\Delta}{=}} Cu + CO$$

$$\Delta_r H_m^\theta = 46.8 \text{ kJ mol}^{-1}$$

$$\Delta_r S_m^\theta = 0.183 \text{ kJ mol}^{-1}$$

$$\Delta_r G_m^\theta (600\ ^\circ\text{C}) = -112.9 \text{ kJ mol}^{-1} < 0$$

Thus, it is a spontaneous reaction. In other words, metallic Cu^0 might be produced through a high-temperature (600 °C) reduction reaction of CuO with carbon. In this sense, the coordination N atoms, reductant carbon, and N_2 atmosphere are three possible key factors for the preparation of metallic Cu^0 supported on ZnO by a simple one-step method.

Usually, CuO supported on ZnO is prepared by homogeneous coprecipitation, deposition–precipitation, and conventional coprecipitation methods. However, to prepare metallic Cu supported on ZnO, the obtained CuO–ZnO composite oxides should be further reduced in H_2 [13,14]. Even when the metallic Cu was used as the copper source to support ZnO, the metallic Cu finally changed to CuO

and the CuO–ZnO composite was formed [15]. In this case, both metallic Cu^0 and ZnO nanoparticles highly dispersed in a carbon substrate are fabricated by a simple one-step pyrolysis process (Scheme 2). Therefore, the method avoids the high-temperature pretreatment under H_2 commonly required for preparation of such Cu–ZnO catalysts.

As shown in Figure 6, Complex shows two stages in the whole pyrolysis process. The first stage is located in the range of 373–460 °C (max exothermic peak at 405.4 °C), which is associated with weight loss of 38.61%. This weight loss should be due to the thermal decomposition of a molecular 1,10-phenanthroline, which is 39.74%, in theory. The second stage shows a slow weight loss (20.68%) from 460 °C to 800 °C, which matches well the theoretical weight loss (21.43%) of an organic group H_3NO_5 from molecular 5-nitroisophthalato. The M–N (M=Cu, Zn, 2.055–2.072 Å) distance is slightly longer than the equatorial M–O (M=Cu, Zn, 1.929–2.015 Å) distance. Thus, 1,10-phenanthroline is removed more easily than the organic group H_3NO_5 of 5-nitroisophthalato. From the above discussion, the sequential thermal decomposition process of Complex is shown as follows:

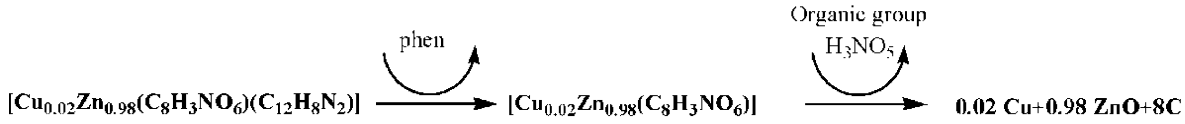

Scheme 2. Pyrolysis steps of Complex under N_2.

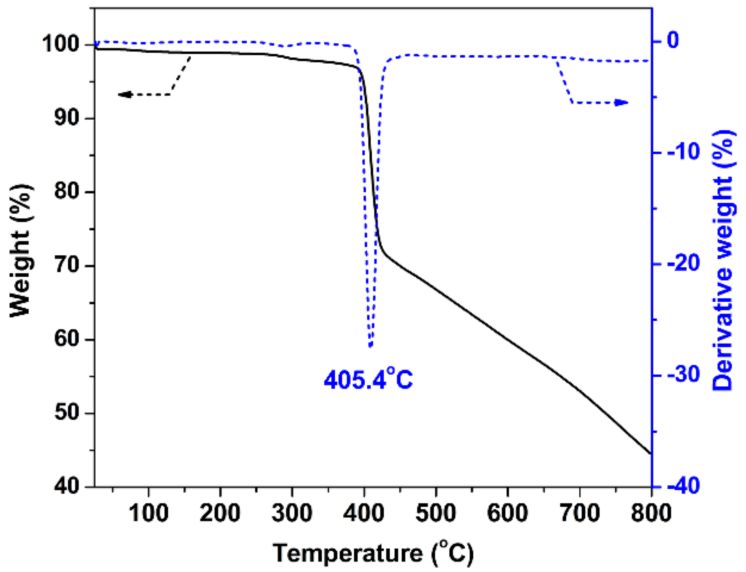

Figure 6. Thermogravimetric curve of Complex under N_2.

3.4. SEM Characterization

Figure 7 shows the SEM images of Cu–ZnO@C from Complex carbonization for 2 h at 600 °C under N_2. It was found that Cu–ZnO@C presents a honeycomb-like pore structure with a coarse outside surface (Figure 7a). As shown in Figure 7c,d, Cu–ZnO@C consists of carbon (79.88 at. %), Cu (0.26 at. %), Zn (10.01 at. %), and O (9.85 at. %) elements. The amount of carbon is much more than that of the other elements. In this sense, the particles presented in the yellow circle of Figure 7b should be the highly dispersed Cu and ZnO particles, and the sufficient carbon should present as the substrate in Figure 7b. Therefore, there are some highly dispersed Cu and ZnO particles decorated on/in the carbon substrate.

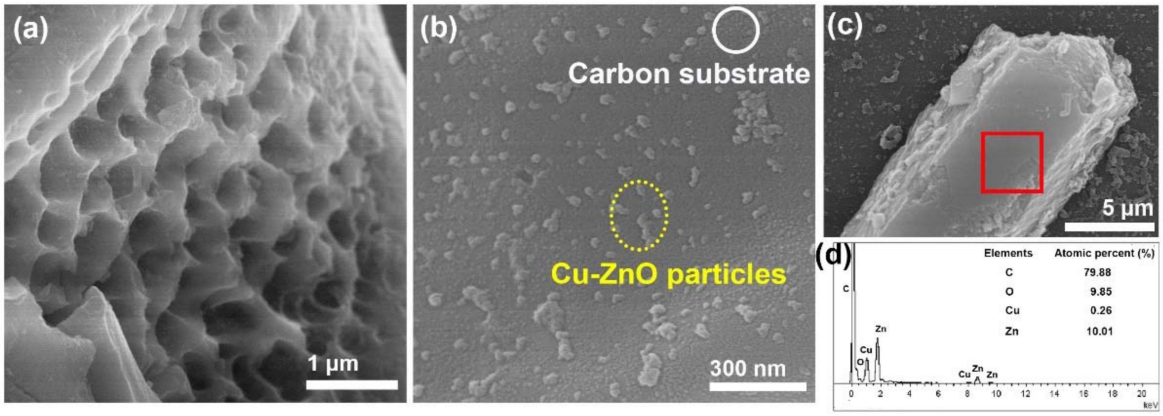

Figure 7. SEM images of the Cu–ZnO@C compound prepared by post-heat-treatment Complex at 600 °C under N_2. (**a**,**c**) Low-resolution image; (**b**) high-resolution image; (**d**) Energy dispersive spectrometer (EDS) spectra recorded from the corresponding red rectangular region in (**c**).

3.5. Measurement of Cu–ZnO@C Composite Catalytic Activity

As stated above, a black Cu–ZnO@C composite has been obtained by a one-step thermal decomposition process, and highly dispersed metallic Cu^0 and ZnO particles can be considered as a heterogeneous catalyst candidate for the typical hydroxylation of benzene to phenol with H_2O_2. The catalytic activities are presented in Table 3. As shown in Entry 1 of Table 3, the as-prepared Complex presented lower benzene conversion (17.3%), phenol selectivity (26.2%), and phenol yield (4.5%). After their calcination at 200 °C (Entry 2, Table 3), these obtained materials also have a similar benzene conversion, phenol yield, and phenol selectivity. According to the results of TGA, Complex had not decomposed at 200 °C. Compared with the control experiment with nonactivation (Entry 8, Table 3), the as-prepared complex presents a certain catalytic activity and phenol selectivity, implying that the as-prepared complex is catalytic under the given condition. Furthermore, with the increase of thermolysis temperature (Entry 3–5, Table 3), the benzene conversion, phenol yield, and phenol selectivity of post-heat-treatment Complex (Cu–ZnO@C composite) obviously increased. In detail, for post-heat-treatment Complex, the benzene conversion, phenol yield, and phenol selectivity reached the maximum values (55.7%, 32.0%, and 57.5%, respectively) with Complex at 600 °C (Entry 5, Table 3). The increased catalytic activities should be derived from more metallic Cu^0 active species because of thermal decomposition. However, with the same component content and valence states, the commercial mixed sample shows much lower benzene conversion, phenol yield, and phenol selectivity (45.6%, 23.1%, and 50.7%, respectively: Entry 7, Table 3). Therefore, the high activities of Cu–ZnO@C composites should be due to highly dispersed metallic Cu^0 and ZnO particles as well as their synergistic interaction. After the maximum, post-heat-treatment Complex at 800 °C (Entry 6, Table 3) presented decreased catalytic activity. Such a high temperature resulted in a serious agglomeration of Cu^0 particles [24], decreasing the specific active area of the Cu^0 particles. As a consequence, the catalytic activity decreased. Therefore, smaller metallic Cu^0 active species will facilitate higher catalytic activity.

To make a more realistic comparison of catalytic activities, turnover frequencies (TOFs) were carefully calculated and compared with the literature data listed in Table 4. Compared with the other candidate catalysts, the TOF of our Cu–ZnO@C catalyst (Entry 1, Table 4) can be ranked at the top. Therefore, our studies present an obvious scientific progress for the catalytic hydroxylation of benzene to phenol. In the future, with increase in the metallic Cu^0 content, the catalytic activities should hopefully be increased.

Table 3. Catalytic activity of the catalysts in the catalytic hydroxylation of benzene to phenol [a].

Entry	Post-Heat-Treatment Temperature (°C)	Benzene Conversion (%)	Phenol Selectivity (%)	Phenol Yield (%)
1	RT [b]	17.3	26.2	4.5
2	200	18.7	27.8	5.2
3	400	30.9	43.3	13.4
4	500	45.6	54.2	24.7
5	600	55.7	57.5	32.0
6	800	49.8	40.8	20.3
7	Commercial mixed sample [c]	45.6	50.7	23.1
8	Without any catalysts	-	-	-

[a] Reaction conditions: 40 mg of catalyst, 1.8 mL (20 mmol) of benzene, 6 mL of 99.8 wt % acetonitrile, 4.1 mL (40 mmol) of 30 wt % H_2O_2, 343 K, 6 h. [b] Room temperature. [c] Made by mixing the commercial metallic Cu^0 (0.7 wt %), ZnO (44.8 wt %), and graphite (54.5 wt %) through mechanical lapping, keeping the same content as that of the Cu–ZnO@C composite.

Table 4. Comparison of the catalytic hydroxylation of benzene to phenol of the reported Cu–ZnO@C catalysts with literature data.

Entry	Catalyst Name	Valence of Main Copper	TOF [a] (mmol mol^{-1} s^{-1})	Ref.
1	Cu–ZnO@C [b]	Cu^0	117.9	This Work
2	TS-1 [c]	-	31.7	[21]
3	CuO–$CuCr_2O_4$	Cu^{2+}	44.9	[25]
4	Cu^{II}-Based complex	Cu^{2+}	22.7	[26]
5	$Cu_{0.09}$-V-HMS	Cu^{2+}	121.9	[27]
6	Cu-g-C_3N_4	Cu^{2+}	1.5	[28]
7	Cu/Ti/HZSM-5	Cu^{2+}/Cu^+	2.0	[29]

[a] Turnover frequency (TOF) = moles of benzene converted (mmol) per one mol of Cu in the catalysts (mol) per one second of reaction time (s). [b] Cu–ZnO@C is the Complex at 600 °C (Entry 5, Table 3). [c] TOF was calculated based on the Ti content of titanium silicalite (TS-1) catalysts.

4. Conclusions

A novel one-dimensional bimetallic complex $[Cu_{0.02}Zn_{0.98}(C_8H_3NO_6)(C_{12}H_8N_2)]_n$ ("Complex") has been successfully synthesized and characterized. Complex was directly pyrolyzed under N_2 to remove organic groups and prepare Cu–ZnO@C composites, which are composed of metallic Cu^0, ZnO, and carbon. One interesting advantage of this simple one-step pyrolysis method is that high-temperature prereduction treatments, which are usually required for Cu–ZnO catalysts, are avoided. The Cu–ZnO@C composite was examined with respect to its catalytic activities for the hydroxylation of benzene to phenol with H_2O_2. The catalytic activities reached the maximum at Complex carbonized at 600 °C, and were higher than that of the commercial mixed sample. The TOF of the Cu–ZnO@C catalyst can be ranked at the top of the communicated candidate catalysts. The highly dispersed metallic Cu^0 and ZnO particles and their synergistic interaction should be responsible for the higher catalytic activities.

Author Contributions: H.W. and L.L. conceived and designed the experiments; G.W. and J.Z. performed the experiments and wrote the manuscript; L.L., Z.Y., and L.S. analyzed the data and modified the paper.

Funding: This research was financially supported by the National Natural Science Foundation of China (21503092, 21501067 and 21773094) and the Natural Science Foundation of Zhejiang Province (LQ18B030006 and LY15B030008).

Conflicts of Interest: The authors declare no conflict of interest.

References

1. Wei, C.; Li, X.; Xu, F.; Tan, H.; Li, Z.; Sun, L.; Song, Y. Metal organic frame work-derived anthill-like Cu@carbon nanocomposites for nonenzymatic glucose sensor. *Anal. Methods* **2014**, *6*, 1550–1557. [CrossRef]
2. Yu, G.; Sun, J.; Muhammad, F.; Wang, P.; Zhu, G. Cobalt-based metal organic frame work as precursor to achieve superior catalytic activity for aerobic epoxidation of styrene. *RSC Adv.* **2014**, *4*, 38804–38811. [CrossRef]
3. McDonald, T.M.; D'Alessandro, D.M.; Krishnac, R.; Long, J.R. Enhanced carbon dioxide capture upon incorporation of *N*,*N*′-dimethylethylenediamine in the metal-organic framework CuBTTri. *Chem. Sci.* **2011**, *2*, 2022–2028. [CrossRef]
4. Sumida, K.; Rogow, D.L.; Mason, J.A.; McDonald, T.M.; Bloch, E.D.; Herm, Z.R.; Bae, T.-H.; Long, J.R. Carbon dioxide capture in metal-organic framework. *Chem. Rev.* **2012**, *112*, 724–781. [CrossRef] [PubMed]
5. Fan, K.-H.; Huang, Q.; Fang, X.-F.; Zhu, L.-W.; Yan, Z. Tuning the spin states of two apical iron(II) ions in a pentanuclear iron(II) cluster helicate through the choice of anions. *Crystals* **2018**, *8*, 119.
6. Chaikittisilp, W.; Ariga, K.; Yamauchi, Y. A new family of carbon materials: Synthesis of MOF derived nanoporous carbons and their promising applications. *J. Mater. Chem. A* **2013**, *1*, 14–19. [CrossRef]
7. Masoomi, M.Y.; Morsali, A. Applications of metal-organic coordination polymers as precursors for preparation of nano-materials. *Coord. Chem. Rev.* **2012**, *256*, 2921–2943. [CrossRef]
8. Liu, B.; Shioyama, H.; Akita, T.; Xu, Q. Metal-organic framework as a template for porous carbon synthesis. *J. Am. Chem. Soc.* **2008**, *130*, 5390–5391. [CrossRef] [PubMed]
9. Li, S.; Xu, Q. Metal-organic frameworks as platforms for clean energy. *Energy Environ. Sci.* **2013**, *6*, 1656–1683. [CrossRef]
10. Radhakrishnan, L.; Reboul, J.; Furukawa, S.; Srinivasu, P.; Kitagawa, S.; Yamauchi, Y. Preparation of microporous carbon fibers through carbonization of Al-based porous coordination polymer (Al-PCP) with furfuryl alcohol. *Chem. Mater.* **2011**, *23*, 1225–1231. [CrossRef]
11. Song, J.; Zhu, C.; Xu, B.; Fu, S.; Engelhard, M.H.; Ye, R.; Du, D.; Beckman, S.P.; Lin, Y. Bimetallic cobalt-based phosphide zeolitic imidazolate framework: CoP_x phase-dependent electrical conductivity and hydrogen atom adsorption energy for efficient overall water splitting. *Adv. Energy Mater.* **2017**, *7*, 1601555. [CrossRef]
12. Zhen, W.; Jiao, W.; Wu, Y.; Jing, H.; Lu, G. The role of interlayer metallic copper for visible photocatalytic hydrogen generation over $Cu/Cu_2O/Cu/TiO_2$ catalyst. *Catal. Sci. Technol.* **2017**, *7*, 5028–5037. [CrossRef]
13. Li, L.; Zhan, Y.; Zheng, Q.; Zheng, Y.; Lin, X.; Li, D.; Zhu, J. Water-gas shift reaction over aluminum promoted Cu/CeO_2 nanocatalysts characterized by XRD, BET, TPR and Cyclic Voltammetry (CV). *Catal. Lett.* **2007**, *118*, 91–97. [CrossRef]
14. Li, L.; Song, L.; Chen, C.; Zhang, Y.; Zhan, Y.; Lin, X.; Zheng, Q.; Wang, H.; Ma, H.; Ding, L.; et al. Modified precipitation processes and optimized copper content of $CuO\text{-}CeO_2$ catalysts for water-gas shift reaction. *Int. J. Hydrogen Energy* **2014**, *39*, 19570–19582. [CrossRef]
15. Li, L.; Song, L.; Wang, H.; Chen, C.; She, Y.; Zhan, Y.; Lin, X.; Zheng, Q. Water-gas shift reaction over CuO/CeO_2 catalysts: Effect of CeO_2 supports previously prepared by precipitation with different precipitants. *Int. J. Hydrogen Energy* **2011**, *36*, 8839–8849. [CrossRef]
16. Li, L.; Zhan, Y.; Chen, C.; She, Y.; Lin, X.; Zheng, Q. Effect of CeO_2 support prepared with different methods on the activity and stability of CuO/CeO_2 catalysts for water-gas shift reaction. *Acta Phys. Chim. Sin.* **2009**, *25*, 1397–1404.
17. Li, D.; Xu, S.; Cai, Y.; Chen, C.; Zhan, Y.; Jiang, L. Characterization and catalytic performance of $Cu/ZnO/Al_2O_3$ water-gas shift catalysts derived from Cu-Zn-Al layered double hydroxides. *Ind. Eng. Chem. Res.* **2017**, *56*, 3175–3210. [CrossRef]
18. Wang, S.; Liu, H. Selective hydrogenolysis of glycerol to propylene glycol on hydroxyl carbonate-derived $Cu\text{-}ZnO\text{-}Al_2O_3$ catalysts. *Chin. J. Catal.* **2014**, *35*, 631–643. [CrossRef]
19. Shi, X.; Yang, X.; Gu, X.; Su, H. CuO-ZnO heterometallic hollow spheres: Morphology and defect structure. *J. Solid State Chem.* **2012**, *186*, 76–80. [CrossRef]
20. Ding, L.; Li, L.; Chen, Y.; Hong, J.; Wang, L.; Hou, J.; Wang, H. Preparation of supported catalysts (CuO/TUD-1,CuO/MCM-41) and their application in one-step oxidation of benzene to phenol. *Chin. J. Synth. Chem.* **2015**, *23*, 300–304.

21. Luo, Y.; Xiong, J.; Pang, C.; Li, G.; Hu, C. Direct hydroxylation of benzene to phenol over TS-1 catalysts. *Catalysts* **2018**, *8*, 49.
22. Sheldrick, G.M. A short history of SHELX. *Acta Crystallogr. Sect. A Found. Crystallogr.* **2008**, *64*, 112–122. [CrossRef] [PubMed]
23. Ren, H.; Song, T.; Xu, J.; He, X.; Wang, L.; Zhang, P.; Ye, J. Self-assembly of two zinc(II) supramolecular architectures with carboxylate and chelating aromatic amine ligands: $[Zn(nba)_2(phen)(H_2O)]$ and $[Zn(nip)(phen)]_n$ (nba = 4-nitrobenzoic acid, nip = 5-nitroisoph thalic acid). *Transit. Met. Chem.* **2006**, *31*, 992–998. [CrossRef]
24. Tanaka, Y.; Kikuchi, R.; Takeguchi, T.; Eguchi, K. Steam reforming of dimethyl ether over composite catalysts of γ-Al_2O_3 and Cu-based spinel. *Appl. Catal. B Environ.* **2005**, *57*, 211–222. [CrossRef]
25. Acharyya, S.; Ghosh, S.; Tiwari, R.; Pendem, C.; Sasaki, T.; Bal, R. Synergistic effect between ultrasmall Cu(II) oxide and $CuCr_2O_4$ spinel nanoparticles in selective hydroxylation of benzene to phenol with air as oxidant. *ACS Catal.* **2015**, *5*, 2850–2858. [CrossRef]
26. Zhang, L.; Qiu, S.; Jiang, G.; Jiang, G.; Tang, R. A Cu-II-based metal-organic framework as an efficient photocatalyst for direct hydroxylation of benzene to phenol in aqueous solution. *Asian J. Org. Chem.* **2018**, *7*, 165–170. [CrossRef]
27. Hu, L.; Yue, B.; Chen, X.; He, H. Direct hydroxylation of benzene to phenol on Cu-V bimetal modified HMS Catalysts. *Catal. Commun.* **2014**, *43*, 179–183. [CrossRef]
28. Muniandy, L.; Adam, F.; Mohamed, A.R.; Iqbal, A.; Rahman, N.R.A. Cu^{2+} coordinated graphitic carbon nitride (Cu-g-C_3N_4) nanosheets from melamine for the liquid phase hydroxylation of benzene and VOCs. *Appl. Surf. Sci.* **2016**, *398*, 43–55. [CrossRef]
29. Ichihashi, Y.; Kamizaki, Y.; Terai, N.; Taniya, K.; Tsuruya, S.; Nishiyama, S. One-Step oxidation of benzene to phenol over Cu/Ti/HZSM-5 Catalysts. *Catal. Lett.* **2010**, *134*, 324–329. [CrossRef]